Clay Minerals, (2018) **53**, 657–663

The effect of calcination temperature on metakaolin structure for the synthesis of zeolites

MAGDALENA KRÓL[1,*] AND PIOTR ROŻEK[1]

[1] *Faculty of Materials Science and Ceramics, AGH University of Science and Technology, 30 Mickiewicza Av., 30-059 Krakow, Poland*

(*Received 24 May 2018; revised 12 August 2018; Accepted Manuscript published online: 17 December 2018; Version of Record published online: 29 January 2019; Associate Editor: J. Labrincha*)

ABSTRACT: The aim of this research was to determine the temperature of kaolin calcination in order to obtain an intermediate product (metakaolin) for the synthesis of geopolymers with potential application as self-supporting zeolitic membranes. The products obtained were analysed with X-ray diffraction (XRD), Fourier-transform infrared (FTIR) spectroscopy and scanning electron microscopy (SEM). The structural analysis of the metakaolins obtained suggested that the optimal temperature for the proposed application is 700°C. After alkali activation of metakaolin, it is possible to obtain zeolite A and hydroxysodalite. The factors analysed, determining the type and quantity of crystalline phases, were activation temperature and concentration of sodium hydroxide solution (activator). The largest amounts of zeolites were obtained by alkali activation with 9 mol/dm^3 NaOH solution at 70°C.

KEYWORDS: kaolin, metakaolin, calcination, alkali activation, geopolymer, self-supported membrane, zeolite A.

Geopolymers are amorphous aluminosilicates that are considered to be the precursors of zeolites. These materials find many applications in chemical technology (Provis & van Deventer, 2009). It was Joseph Davidovits who, in the 1970s, introduced the term 'geopolymer' and its definition for materials synthesized by the reaction of aluminosilicate powders with alkaline solutions (activators) at temperatures <100°C (Davidovits, 1991). Numerous attempts have been made to obtain geopolymers from Si- and Al-rich industrial wastes and by-products (*e.g.* fly ash, silica fume, slag, red mud [residue from the production of aluminium] and amorphous metakaolin; Provis & van Deventer, 2009).

The structure and properties of geopolymers depend mainly on the starting raw material. The quality of geopolymer is also affected by the type and concentration of alkaline activator, activation temperature and time of polycondensation. Hydroxides and silicates of alkali metals (sodium and potassium) are commonly used activators (Xu & van Deventer, 2000). Geopolymers exhibit high compressive strength (>90 MPa after 28 days) and flexural strength (10–15 MPa), resistance to changing weather conditions, low porosity and little binding shrinkage (<0.05%) (Davidovits, 2016). The synthesis of metakaolin- and fly ash-based geopolymers resistant to fire, frost, acids, sulfates and seawater has also been studied (Fernandez-Jimenez & Palomo, 2005).

Metakaolin is the anhydrous calcined form of the clay mineral kaolinite, often examined in the context of the starting material for the production of geopolymers or as a pozzolanic additive to Portland cement. The optimum activation temperatures range from 550°C to 850°C (Snellings *et al.*, 2012). Kakali *et al.* (2001) calcined kaolins at 650°C for 3 h and reported that the

*E-mail: mkrol@agh.edu.pl
https://doi.org/10.1180/clm.2018.49

pozzolanic activity of the metakaolin produced from dehydroxylated disordered kaolinite was greater than that of metakaolin from ordered kaolinite. Abo-El-Enein *et al.* (2014) prepared metakaolin by firing kaolin at 750–825°C for 2 h. The optimum firing temperature of metakaolin with respect to the pozzolanic activity with hydrated lime as an activator was 750°C. Kenne Diffo *et al.* (2015) studied the effect of the calcination rate (in the range 1–20°/min to 700°C) of kaolin on the mechanical properties of metakaolin-based geopolymers and reported that lower calcination rates resulted in more durable materials. Zuhua *et al.* (2009) calcined kaolin at 600–1000°C for 6 h and tested the strength of the calcined geopolymers. However, those authors did not confirm the presence or absence of zeolites in the geopolymeric matrix, although geopolymers are considered to be precursors of zeolites (Liu *et al.*, 2016).

Geopolymers incorporating zeolites may merge interesting properties of both aluminosilicate materials. While geopolymeric gel serves as a support for zeolites, zeolites provide greater surface area, porosity and cation exchange capacity (Khalid *et al.*, 2018). Geopolymer–zeolite composites may be used as self-supporting membranes (Zhang *et al.*, 2014) or solid adsorbents of carbon dioxide (Minelli *et al.*, 2018). Geopolymer–zeolite composites may be obtained by adding a commercial zeolite (*e.g.* zeolite Na13X) to a geopolymer slurry at the stage of mixing (Papa *et al.*, 2018) or by hydrothermal treatment of a solid geopolymer (Wang *et al.*, 2018). Zeolites A and X may also form in the metakaolin-based geopolymer matrix by simple curing in an autoclave at elevated temperatures, without applying hydrothermal treatment (Król *et al.*, 2016; Brylewska *et al.*, 2018). In fly ash-based geopolymers, the most commonly present zeolite-like phase is hydroxysodalite (Rożek *et al.*, 2018).

The aim of this research was to characterize the structure of metakaolin-based materials. Due to the various temperatures of metakaolin production for application as a raw material in alkali activation used in previous studies, the reactivity of metakaolin obtained at various temperatures was assessed. The optimum firing temperature of metakaolin in the context of zeolite synthesis was analysed for the first time. In addition, diffuse reflectance infrared Fourier-transform spectroscopy (DRIFTS) was used to analyse structural changes during heating of the kaolinite sample. The influence of geopolymerization temperature and activator concentration on the type of zeolite phases obtained was also investigated.

MATERIALS AND METHODS

Starting material

Kaolin KOC (Surmin-Kaolin) was used as the starting material. Homogenized samples of the kaolin were thermally treated at 600°C, 700°C and 800°C for 2 h (temperatures were chosen on the basis of literature data and DRIFTS measurements) to obtain metakaolin. The metakaolin materials were named as ME600, ME700 and ME800, respectively.

Alkali activation

The metakaolin materials obtained in calcination process were subjected to alkali activation. For this purpose, metakaolin specimens were mixed with aqueous solutions of 3, 5, 7 and 9 mol/dm^3 NaOH at a 0.8:1.0 solution:solid ratio. The slurries were inserted into silicon moulds under vibration to exclude air bubbles. Because polycondensation during the geopolymerization process is not spontaneous but demands energy (Xu & van Deventer, 2000), the samples were sealed with plastic film and put into a laboratory dryer for 24 h at 70°C and 90°C activation temperatures.

Methodology

Phase composition was determined by XRD from International Centre for Diffraction Data (ICDD)-registered mineral patterns with a Philips X-ray diffractometer X'Pert system (Cu-*K*α radiation). The XRD patterns were obtained in the range 5–60°2θ, with a step 0.05°2θ and 2 s per step.

The FTIR spectra were obtained with a Bruker VERTEX 70v vacuum spectrometer in the mid-infrared range (4000–400 cm^{-1}). The samples were prepared by the KBr (Merck) method. Spectra were recorded in absorbance mode with 128 scans and a resolution of 4 cm^{-1}. The same spectrometer equipped with a diffuse reflectance cell (Praying Mantis™ with a reaction chamber and temperature controller) was used to obtain *in situ* DRIFT spectra of the kaolin heated at 700°C. Spectra were collected at 2 min (every 10°C) intervals in the range 4000–600 cm^{-1} over 64 scans and at 4 cm^{-1} resolution.

The chemical compositions of kaolin and the calcination products were determined by X-ray fluorescence (XRF). A WD-XRF spectrometer (Axios mAX 4 kW, PANalytical, The Netherlands) equipped with Rh source was used to determine the concentrations of elements. Microstructure analysis of the materials was

https://doi.org/10.1180/clm.2018.49 Published online by Cambridge University Press

performed with an FEI Nova Nanosem 200 scanning electron microscope on graphite-coated samples.

RESULTS AND DISCUSSION

The XRD trace of the starting kaolin is shown in Fig. 1. The sample contains quartz and minor muscovite impurities except for kaolinite. The chemical compositions of kaolin and its calcination products are listed in Table 1.

Heating of kaolin results in partial decomposition and structure rearrangement due to the removal of water in the crystal lattice of kaolinite (at 500–800°C dehydroxylation) (Bolewski & Żabiński, 1979; Osornio-Rubio *et al.*, 2016). These reactions may be theoretically denoted as shown in reaction 1:

$$Al_4[Si_4O_{10}](OH)_8 \rightarrow Al_4[Si_4O_{13}](OH)_2 + 3H_2O \rightarrow Al_4[Si_4O_{14}] + H_2O \quad (1)$$

The calcination temperature of kaolin was determined with DRIFTS, which allows *in situ* temperature measurement. The spectra obtained are shown in Fig. 2. For readability, only some records are presented at temperature intervals of 50°C. From 600°C, rapid dehydroxylation is observed as a clear change in the range of OH-stretching vibrations (*i.e.* 3800–3600 cm^{-1}), and this is combined with an amorphization of structure (Si–O vibrations at 1200–600 cm^{-1}). Therefore, for further research, temperatures of 600°C, 700°C and 800°C were chosen.

The products of kaolin calcination at 600°C, 700°C and 800°C were examined by XRD (Fig. 3). Kaolinite, the dominant phase in the starting material, was transformed completely into the amorphous phase. Only in the ME600 sample did kaolinite remain, as is indicated by the persistence of the peak at 12.4°2θ. In all of the patterns, a hump appeared in the range 20–30°2θ, which indicates amorphization of the kaolin. Peaks related to quartz and muscovite present in the starting material (Fig. 1) were also observed in the fired products (Fig. 3).

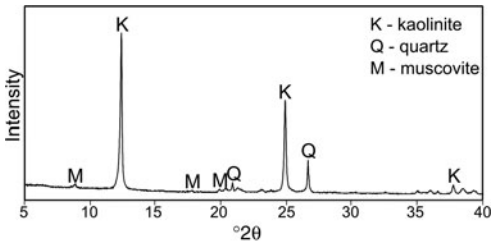

FIG. 1. XRD pattern of kaolin KOC.

TABLE 1. Chemical composition (wt.%) of the original kaolin (KOC) and the metakaolins (ME) fired at various temperatures.

Sample	KOC	ME600	ME700	ME800
SiO_2	57.75	53.56	53.51	53.91
TiO_2	0.65	0.48	0.49	0.51
Al_2O_3	39.41	44.18	44.13	43.66
Fe_2O_3	0.55	0.41	0.43	0.43
CaO	0.08	0.06	0.09	0.07
MgO	0.15	0.17	0.17	0.18
Na_2O	0.06	0.08	0.10	0.08
K_2O	0.69	0.55	0.56	0.60
P_2O_5	0.28	0.23	0.24	0.24
SO_3	0.09	0.05	0.05	0.05
Other	0.29	0.23	0.23	0.27

The FTIR spectra of metakaolins obtained at various temperatures are shown in Fig. 4. In all of the spectra, the main infrared bands may be assigned as follows:

- The bands at 1086–1099 cm^{-1} result from asymmetric stretching vibrations of Si–O–(Si, Al) bonds.
- The doublet at 800 and 780 cm^{-1}, which is related to symmetrical Si–O–Si stretching vibrations, is characteristic of quartz.
- The bands at ~695 cm^{-1} are attributed to Al–O–Si symmetric stretching vibrations.
- The bands at ~469 cm^{-1} are related to bending Si–O–Si(Al) vibrations.

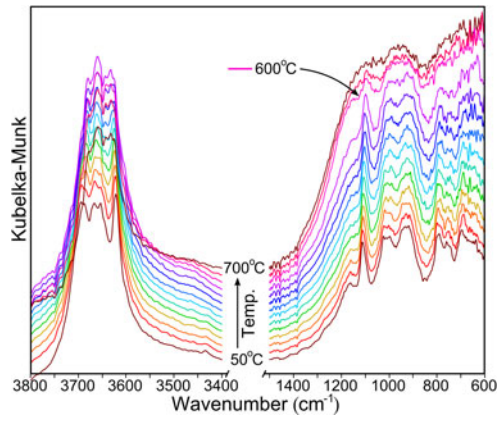

FIG. 2. DRIFT spectra of kaolin recorded at 50°C intervals.

https://doi.org/10.1180/clm.2018.49 Published online by Cambridge University Press

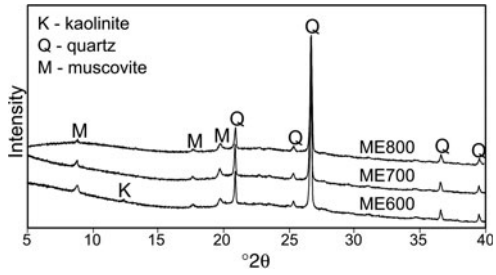

FIG. 3. XRD traces of metakaolins obtained at various temperatures.

– Finally, in ME700 and ME800, the band at 567 cm^{-1} is attributed to the vibrations of rings built of [TO_4] tetrahedra (Mozgawa *et al.*, 2006), as well as to octahedral Al–O vibrations (Tarte, 1967).

Scanning electron micrographs of the metakaolins are shown in Fig. 5. The thermal treatment modified the clay microstructure in comparison to the starting kaolin (Fig. 5a). Kaolinite crystals have a pseudohexagonal habit and form characteristic aggregates that arrange into booklets (Christidis, 2011). The least structural modification was observed in ME600 (Fig. 5b); despite the fact that the crystal size decreased, some of the crystals remained unchanged, retaining the initial habit of hexagonal plates. In samples ME700 (Fig. 5c) and ME800 (Fig. 5d),

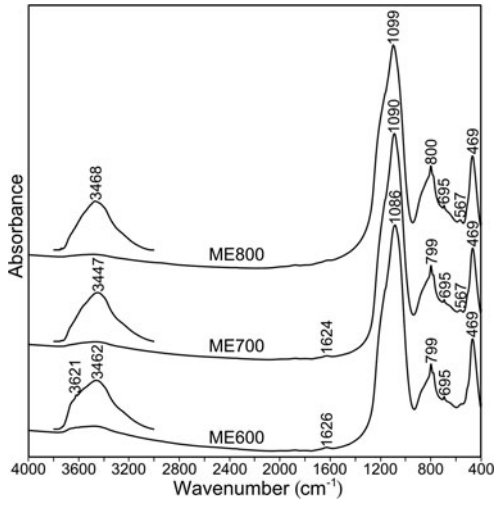

FIG. 4. FTIR spectra of metakaolins collected at various temperatures.

amorphization was observed, which was confirmed by detailed analysis of the infrared spectra (Fig. 4). Indeed, the OH-stretching vibrations of kaolinite bands at 3696, 3669, 3653 and 3621 cm^{-1} with low integral intensity (Król *et al.*, 2016) may be observed only in the spectrum of ME600 (clearly visible when enlarging this part of the spectrum). In contrast, significant differences in the microstructures of ME700 (Fig. 5c) and ME800 (Fig. 5d) were not observed.

The data obtained suggest that a temperature of 600°C is too low to cause complete transformation of kaolin into metakaolin. However, the firing products at 700°C and 800°C were essentially X-ray amorphous, containing only minor crystalline phases such as quartz and muscovite.

The next step was to assess the influence of the activation temperature on the reactivity of the metakaolin during alkali activation with various concentrations of NaOH. X-ray diffraction was used to determine the phase compositions of samples obtained during alkali activation, and the results are presented in Fig. 6. Beside quartz and clay mica, which were present in the starting material (Fig. 1), zeolite A and hydroxysodalite were identified. In those samples activated at 70°C (Fig. 6a), the zeolite formed was obtained at the highest concentration of NaOH used (9 mol/dm^3), but only in metakaolins prepared at lower temperatures. Therefore, ME700 was most active, while only amorphous matter was obtained from ME800. Thus, the temperature of 700°C was optimal for obtaining an intermediate product with potential application in sorption processes. Synthesis of zeolite proceeds in several stages, with the first being the dissolution of the aluminosilicate raw material (Cundy & Cox, 2005). The metakaolin obtained at 700°C is probably subjected to this process to a greater extent and, consequently, the successive stages of the formation of zeolite structures may occur.

Alkali activation at 90°C yielded various results. Upon activation with 9 M NaOH solution, all metakaolins yielded zeolites. ME600 yielded the largest amounts of zeolite. ME700, in turn, produced zeolites with the lowest concentration of activator (7 M NaOH). As a general trend, alkali activation at 90°C favours the formation of sodalite, which has inferior sorption properties.

Figure 7 shows the infrared spectra of materials produced from ME600 after alkali activation at 70°C. The bands attributed to Si–O vibrations are observed in the range of 1000–400 cm^{-1}. Because zeolite phases are present in the analysed samples, the infrared region

https://doi.org/10.1180/clm.2018.49 Published online by Cambridge University Press

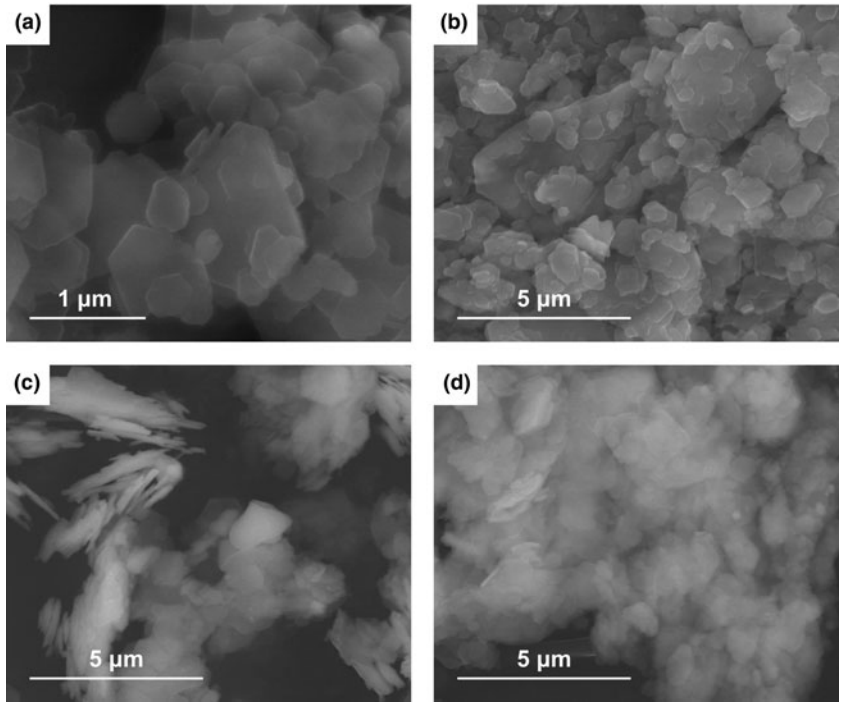

FIG. 5. SEM images of KOC (a), ME600 (b), ME700 (c) and ME800 (d).

of 800–500 cm^{-1} enables the observation of bands due to ring vibrations (Mozgawa, 2007). A characteristic structural unit for zeolite A is the double four ring, with absorption bands at ~560 cm^{-1}. The occurrence of these bands in ME600 activated at 70°C with 9 M NaOH (Fig. 7) confirms that the largest amount of zeolite is obtained by using the highest concentration of NaOH. In addition, the full width at half maximum

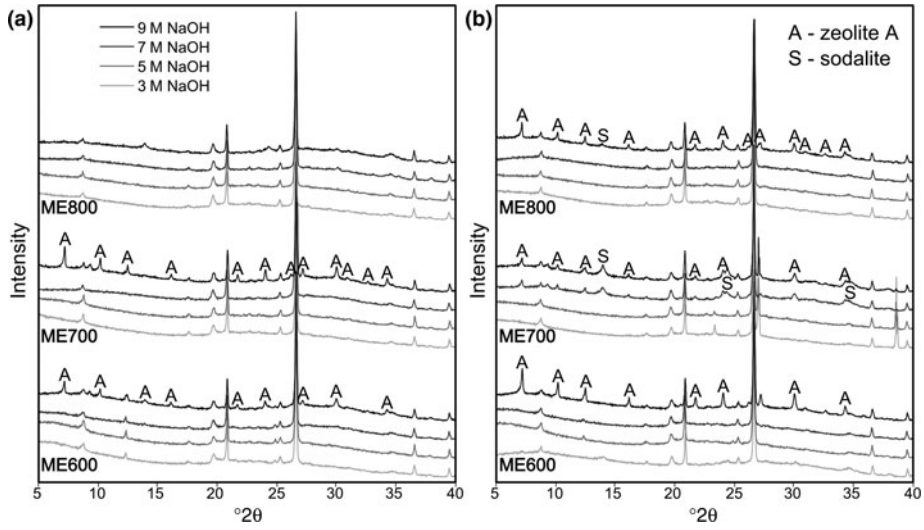

FIG. 6. XRD traces of the alkali-activated metakaolins at (a) 70°C and (b) 90°C.

https://doi.org/10.1180/clm.2018.49 Published online by Cambridge University Press

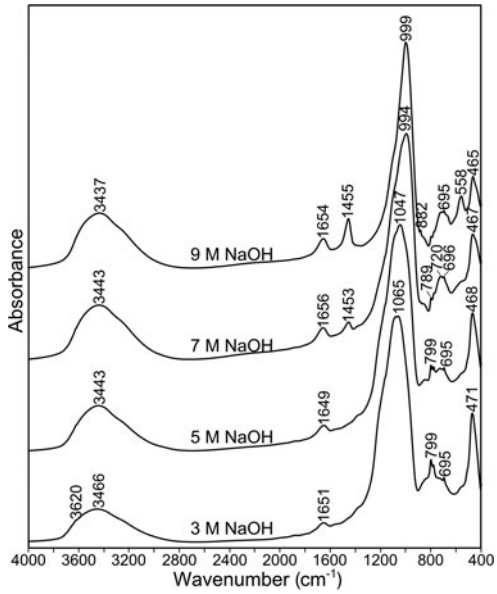

FIG. 7. FTIR spectra of alkali-activated ME600 at 70°C at various NaOH concentrations.

of bands corresponding to the Si–O vibrations decreases with increasing abundance of the crystalline phases. The intensity of the band at ~1455 cm^{-1}, assigned to the vibrations of carbonate groups, increases with increasing concentration of NaOH. This band is related to the reaction of NaOH with atmospheric CO_2 during thermal activation at elevated temperature. Finally, the intense band at 3460 cm^{-1} due to O–H stretching, and the corresponding O–H bending vibrations at 1650 cm^{-1}, indicate the presence of adsorbed – mostly zeolitic – water in the analysed samples. The spectra of the remaining samples are similar to sample ME600 (data not shown) and are in accordance with their mineralogical composition (Fig. 6).

CONCLUSIONS

The following conclusions can be drawn from this study:

- The DRIFT spectra used to observe changes in kaolinite structure during firing at >600°C showed rapid dehydroxylation and structure amorphization, indicating transformation of kaolinite into metakaolinite.
- The most active metakaolin for zeolite synthesis by alkali activation was obtained after calcination at 700°C.
- Optimum synthesis conditions yielded zeolite A in an amorphous matrix of geopolymer. Such composites may be used as self-supporting zeolitic membranes.
- The largest amounts of zeolites might be obtained by alkali activation of ME600 and ME700 with 9 mol/dm^3 NaOH solution at 70°C and ME600 with 9 mol/dm^3 solution at 90°C.
- The increase in activation temperature favours hydroxysodalite, which does not have a disadvantageous structure for sorption applications.

ACKNOWLEDGEMENTS

This work was financially supported by the National Science Centre in Poland under grant no. 2015/17/B/ST8/01200.

REFERENCES

Abo-El-Enein S.A., Amin M.S., El-Hosiny F.I., Hanafi S., ElSokkary T.M. & Hazem M.M. (2014) Pozzolanic and hydraulic activity of nano-metakaolin. *HBRC Journal*, **10**, 64–72.

Bolewski A. & Żabiński W. (1979) *Metody Badań Minerałów i Skał* (in polish). Wydawnictwa Geologiczne, Kraków, Poland.

Brylewska K., Rożek P., Król M. & Mozgawa W. (2018) The influence of dealumination/desilication on structural properties of metakaolin-based geopolymers. *Ceramics International*, **44**, 12853–12861.

Christidis G.E. (2011) Industrial clays. Pp. 341–414 in: *Advances in the Characterization of Industrial Minerals* (G.E. Christidis, editor). EMU Notes in Mineralogy, **9**, European Mineralogical Union and the Mineralogical Society of Great Britain & Ireland, London.

Cundy C.S. & Cox P.A. (2005) The hydrothermal synthesis of zeolites: precursors, intermediates and reaction mechanism. *Microporous and Mesoporous Materials*, **82**, 1–78.

Davidovits J. (1991) Geopolymers – inorganic polymeric new materials. *Journal of Thermal Analysis*, **37**, 1633–1656.

Davidovits J. (2016) *Geopolymer Chemistry and Applications*. www.geopolymer.org

Fernandez-Jimenez A. & Palomo A. (2005) Chemical durability of geopolymers. Pp. 167–193 in: *Geopolymer, Green Chemistry and Sustainable Development Solutions* (J. Davidovits, editor). Geopolymer Institute, Saint-Quentin, France.

https://doi.org/10.1180/clm.2018.49 Published online by Cambridge University Press

Kakali G., Perraki T., Tsivilis S. & Badogiannis E. (2001) Thermal treatment of kaolin: the effect of mineralogy on the pozzolanic activity. *Applied Clay Science*, **20**, 73–80.

Kenne Diffo B.B., Elimbi A., Cyr M., Dika Manga J. & Tchakoute Kouamo H. (2015) Effect of the rate of calcination of kaolin on the properties of metakaolin-based geopolymers. *Journal of Asian Ceramic Societies*, **3**, 130–138.

Khalid H.R., Lee N.K., Park S.M., Abbas N. & Lee H.K. (2018) Synthesis of geopolymer-supported zeolites *via* robust one-step method and their adsorption potential. *Journal of Hazardous Materials*, **353**, 522–533.

Król M., Minkiewicz J. & Mozgawa W. (2016) IR spectroscopy studies of zeolites in geopolymeric materials derived from kaolinite. *Journal of Molecular Structure*, **1126**, 200–206.

Liu Y., Yan C., Zhang Z., Gong Y., Wang H. & Qiu X. (2016) A facile method for preparation of floatable and permeable fly ash-based geopolymer block. *Materials Letters*, **185**, 370–373.

Minelli M., Papa E., Medri V., Miccio F., Benito P., Doghieri F. & Landi E. (2018) Characterization of novel geopolymer – zeolite composites as solid adsorbents for CO_2 capture. *Chemical Engineering Journal*, **341**, 505–515.

Mozgawa W., Jastrzębski W. & Handke M. (2006) Cation-terminated structural clusters as a model for the interpretation of zeolite vibrational spectra. *Journal of Molecular Structure*, **792–793**, 163–169.

Mozgawa W. (2007) *Spektroskopia Oscylacyjna Zeolitów* (in polish). Wydawnictwa AGH, Kraków, Poland.

Osornio-Rubio N.R., Torres-Ochoa J.A., Palma-Tirado M.L., Iménez-Islas H.J., Rosas-Cedillo R., Fierro-Gonzalez J.C. & Martínez-González G.M. (2016) Study of the dehydroxylation of kaolinite and alunite from a Mexican clay with DRIFTS-MS. *Clay Minerals*, **51**, 55–68.

Papa E., Medri V., Amari S., Manaud J., Benito P., Vaccari A. & Landi E. (2018) Zeolite–geopolymer composite materials: production and characterization. *Journal of Cleaner Production*, **171**, 76–84.

Provis J.L. & van Deventer J.S.J. (2009) *Geopolymers: Structure, Processing, Properties and Industrial Applications*. Woodhead Publishing, Abingdon, UK.

Rożek P., Król M. & Mozgawa W. (2018) Spectroscopic studies of fly ash-based geopolymers. *Spectrochimica Acta Part A: Molecular and Biomolecular Spectroscopy*, **198**, 283–289.

Snellings R., Mertens G. & Elsen J. (2012) Supplementary cementitious materials. *Reviews in Mineralogy and Geochemistry*, **74**, 211–278.

Tarte P. (1967) Infra-red spectra of inorganic aluminates and characteristic vibrational frequencies of AlO_4 tetrahedra and AlO_6 octahedra. *Spectrochimica Acta Part A: Molecular Spectroscopy*, **23**, 2127–2143.

Wang H., Yan C., Li D., Zhou F., Liu Y., Zhou C. & Komarneni S. (2018) In situ transformation of geopolymer gels to self-supporting NaX zeolite monoliths with excellent compressive strength. *Microporous and Mesoporous Materials*, **261**, 164–169.

Xu H. & van Deventer J.S.J. (2000) The geopolymerisation of alumino-silicate minerals. *International Journal of Mineral Processing*, **59**(3), 247–266.

Zhang J., He Y., Wang Y., Mao J. & Cui X. (2014) Synthesis of a self-Supporting faujasite zeolite membrane using geopolymer gel for separation of alcohol/water mixture. *Materials Letters*, **116**, 167–170.

Zuhua Z., Xiao Y., Huajun Z. & Yue C. (2009) Role of water in the synthesis of calcined kaolin-based geopolymer. *Applied Clay Science*, **43**, 218–223.

https://doi.org/10.1180/clm.2018.49 Published online by Cambridge University Press